Review Article

Polymer/QDs Nanocomposites for Waveguiding Applications

H. Gordillo, I. Suárez, R. Abargues, P. Rodríguez-Cantó, S. Albert, and J. P. Martínez-Pastor

(Unidad Asociada al CSIC-IMM) UMDO, Instituto de Ciencia de los Materiales, Universidad de Valencia, P.O. Box 22085, 46071 Valencia, Spain

Correspondence should be addressed to I. Suárez, isaac.suarez@uv.es

In this paper we review our recent progress in a still young type of active waveguides based on hybrid organic (polymer)—inorganic (semiconductor quantum dots) materials. They can be useful for the implementation of new photonic devices, because combining the properties of the semiconductor nanostructures (quantum size carrier confinement and temperature independent emission) with the technological capabilities of polymers. These optical waveguides can be easily fabricated by spin-coating and UV photolithography on many substrates (SiO_2/Si, in the present work). We demonstrate that it is possible to control the active wavelength in a broad range (400–1100 nm), just by changing the base quantum dot material (CdS, CdSe, CdTe and PbS, but other are possible), without the necessity of changing fabrication conditions. Particularly, we have determined the optimum conditions to produce multi-color photoluminescence waveguiding by embedding CdS, CdSe and CdTe quantum dots into Poly(methyl methacrylate). Finally, we show new results regarding the incorporation of CdSe nanocrystals into a SU-8 resist, in order to extrapolate the study to a photolithographic and technologically more important polymer. In this case ridge waveguides are able to confine in 2D the light emitted by the quantum dots.

1. Introduction

Research is evolving toward the design of novel functional materials to perform more complex and efficient tasks. One of the most promising approaches is the incorporation of nanoparticles into a host matrix to form a nanocomposite [1]. These synthetic multicomponent materials have an important concern nowadays because they combine the novel properties of semiconducting, metallic and magnetic nanoparticles (e.g., quantum confinement, surface plasmon resonance, superparamagnetism, resp.) with those provided by the matrix. For this purpose the choice of polymers as a host matrix is an attractive approach because they are cheap, flexible, and can be easily processed into films on a great variety of substrates. Moreover, some polymers can be micro- and nanopatterned by different lithographic techniques such as nanoimprint, electron beam, and ultraviolet lithography [2]. This is of significant importance for the fabrication of photonic nanostructures and more complex devices.

The incorporation of optically active materials such as organic dyes [3], rare earth ions [4], semiconducting [5], and metal nanoparticles [6] into polymers has found multitude of applications in optical amplification [7], photovoltaics [8], photodetection [9], sensing [10], and plasmonics [11]. Among these wide range of applications, polymers are especially suitable materials for waveguiding in integrated optic devices, because of its high transparency above 400 nm, low propagation losses, and easy fabrication [12]. In this sense, polymer-based nanocomposites can be good candidates for active waveguiding applications by embedding semiconducting nanocrystals synthesized by colloidal chemistry [13]. These nanocrystals are usually known as quantum dots (QDs), due to the three-dimensional size confinement of carriers. As a result, the effective bandgap of QDs and hence their photoluminescence (PL) can be tuned by either modifying their radius [14] or the composition: CdS [15], CdSe [16], and CdTe [17] in the visible spectra and PbS [18], PbSe [19], and InAs [20] in the near infrared. QDs has been incorporated in sol-gel oxide waveguides to develop optical amplification [21], but also in PMMA to implement a microcavity laser [22] or to amplify the spontaneous emission [23]. In a recent paper, we have demonstrated multicolor waveguiding by dispersing CdSe ($\lambda_{PL} = 600$ nm) and CdTe ($\lambda_{PL} = 550$ nm) QDs into a PMMA-based planar waveguide

[24]. We tested different nanocomposite formulation to obtain the optimum concentration of QDs in the film for waveguiding.

In this paper, we review our recent progress in the development of QDs-PMMA nanocomposite waveguides. New active planar waveguides covering a broad range of the light spectrum from 400 to 1100 nm, are implemented by embedding different types of QDs (CdS, CdTe, CdSe, and/or PbS) into PMMA matrix. These nanocomposites constitute the core of a planar waveguide when they are deposited on a material with lower refractive index, in our case a SiO_2 thin film over a Si substrate. It is interesting to say that the optimum conditions for low propagation losses can be extrapolated from one QD material to another without changing the concentrations or the functionalization of the QD. Then, a new method for developing active multicolor waveguiding in integrated photonic devices is proposed. Finally, new results of the dispersion of CdSe QDs in a SU-8 photoresist are presented. The choice of this resist comes from its interesting photolithographic properties and high refractive index. However, for the dispersion of QDs in SU8, it is necessary the modification of their solubility, which was achieved by means of a ligand exchange procedure. After it, straight ridges can be defined by means of UV-photolithography on the SiO_2/Si substrate coated with the QD-SU8 nanocomposite. We show that these structures are able to guide CdSe PL in two dimensions, revealing the potentiality and promising applications of these new materials in integrated optic devices.

2. Samples Preparation and Experimental Setup

The core of the waveguides used in this work consisted of different sorts of QDs (CdS, CdSe, CdTe, and PbS) embedded in a PMMA matrix. The QDs have different compositions and size, so they will lead to optical transitions at different wavelengths. They were synthesized following the procedure developed by Peng's group [25] using oleic acid as a capping agent, and then mixed with PMMA. For this purpose both the polymer and the QD were dissolved in toluene as a common solvent, in order to obtain a homogeneous dispersion of QDs in the resulting film. The concentration of QDs into the matrix has been adjusted according to our previous results [24], where an optimum filling factor between 10^{-3} and 10^{-4} was found to achieve an optimum waveguiding.

Once the nanocomposites were properly formulated, waveguides were fabricated by spin-coating the solution on a SiO_2/Si substrate and baked between 80 and 150°C for 2 minutes. The final film thickness was around 1 and 2 μm in the waveguides emitting in the visible (CdS, CdSe, and CdTe) and in the IR (PbS), respectively. The choice of the substrate was due to two reasons. First, the low refractive index of SiO_2 (around 1.458 at 600 nm) with respect to the PMMA (around 1.489 at 600 nm) provides a high refractive index contrast (~2%), required for a good confinement of the light in the core of the waveguide. Second, the silicon substrate makes the structure compatible with microtechnology techniques.

The necessary thicknesses of the SiO_2 cladding depend on the wavelength of the light. The wafers used in the waveguides emitting in the IR had a SiO_2 thickness of 2 μm and were supplied by Cimat Silicon SA. The substrates chosen for the waveguides emitting in the visible range were fabricated in our laboratory by spin-coating a H_2O-EtOH acid solution of tetraethyl orthosilicate (TEOS) on a silicon wafer and baking around 300°C during 5 minutes. The resulting film had a thickness of around 0.6 μm. Finally, the edges of the samples were cleaved for end-fire coupling purposes. The inset of Figure 1 shows the structure of the planar waveguides.

PL experiments have been carried out by pumping the colloidal (or nanocomposite) solution dropped in a glass with a 404 nm GaN laser. Then, backscattered PL is collected with the aid of a lens to a fiber optic connected to either a StellarNet EPP2000 or Ocean Optics spectrographs. Absorption spectra of QD colloidal solutions were measured by using a Shimadzu UV-2501PC spectrophotometer (UV-visible range) or an Ocean Optics spectrograph plus a filtered halogen lamp (near-infrared light). Absorption spectra of nanocomposite thin films have been characterized using a Nanocalc 2000 reflectometer (from Mikropack) or an IR Ocean Optics spectrograph by spin-coating the film solution in a glass substrate. Finally, PL waveguiding has been characterized by end fire coupling a 404 nm GaN diode laser and a 633 nm HeNe laser with the aid of a microscope objective at the input edge of the waveguide (see Figure 1). The output light is collected by another microscope objective to perform imaging with a CCD camera or to analyze PL by coupling into the entry fiber optics of the appropriate spectrograph. When planar waveguides were analyzed, a cylindrical lens was used to focus its linear modal distribution to a spot into the collecting optical fiber. Furthermore, PL waveguiding has been also achieved and measured by laser pumping from the top surface of the samples using a cylindrical lens (see dashed rectangle frame in Figure 1) that focus the laser beam into a line segment.

3. QD Emission and Absorption

PL and absorption properties of the QDs have a direct dependence on the radius and composition. Figures 2 and 3 show the absorption and PL spectra of the colloidal QDs used in this work. Four different types of nanocrystals have been synthesized to fabricate the waveguides: CdS, CdTe, and CdSe for visible (Figure 2), and PbS for near infrared (Figure 3).

Figure 2 shows the absorption (Figure 2(a)) and PL (Figure 2(b)) spectra of the three QDs emitting in the visible. The exciton peak in the absorption spectra is placed at 447, 537, and 580 nm for CdS, CdTe, and CdSe, respectively. For longer wavelengths the absorption decreases, arriving to a value close to zero for wavelengths shifted 100 nm beyond the exciton peak. At shorter wavelengths the absorbance increases, and some excited state optical transitions are observed. According to the data reported by other authors [26], these exciton transitions correspond to a QD radius of 4.5 nm for CdS, 1.5 nm for CdTe, and 2.5 nm for CdSe. The PL spectra of the QDs (colloidal or nanocomposite
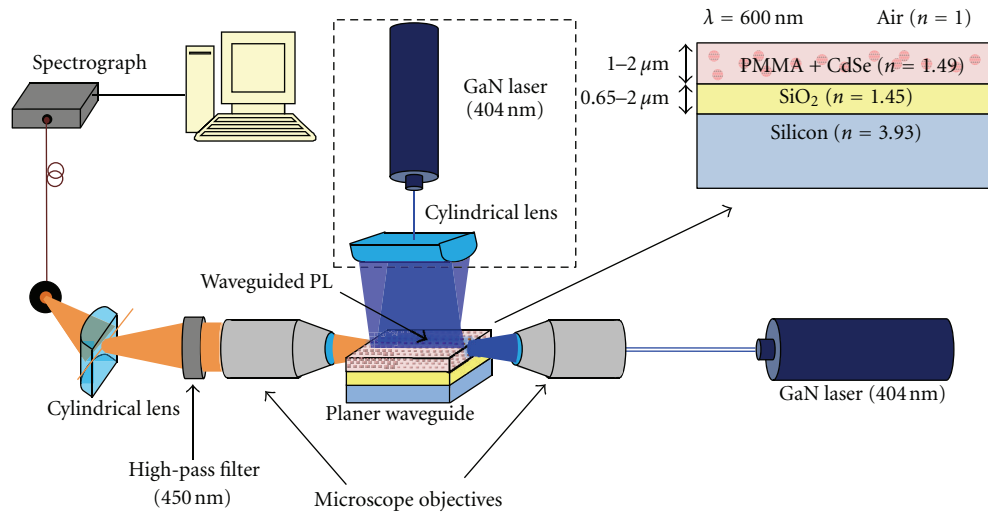
FIGURE 1: Experimental setup for characterizing the waveguides. The inset shows the structure of the waveguides.

(a)

(b)
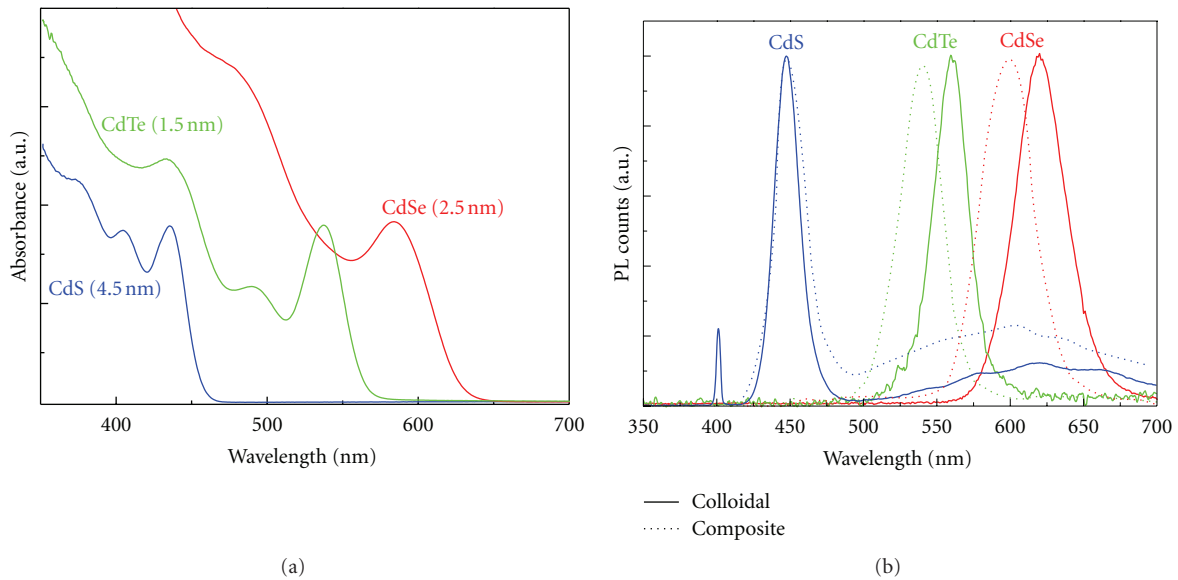
FIGURE 2: Absorption (a) and PL spectra (b) of colloidal CdS (blue), CdTe (green), and CdSe (red) QDs. Dotted lines correspond to PL spectra in the PMMA/NQD nanocomposite.

solutions) consist of single Gaussian lines slightly red-shifted with respect to the exciton peak in absorption by about 40 nm, which is known as Stokes shift [27]. The (FWHM) full width at half maximum of the PL lines decreases with the emission wavelength, being it around 20, 30, and 40 nm for the CdS, CdTe and CdSe, respectively, indicating that size dispersion changes accordingly. In the case of CdS QDs, a broad PL band is observed at around 620 nm that is attributed to carriers trapped at surface states [5]. Finally, dotted lines in Figure 2(b) depict the emission spectra of QD-PMMA nanocomposite solutions for the three materials. The spectra have a similar shape as the colloidal solution, but a larger Stokes shift is observed for CdSe and CdTe QDs, probably due to the presence of nanoparticle aggregates [28].

Figure 3 shows absorption and PL spectra of PbS QDs used in this work. The exciton peak is placed at 960 and 1020 nm in absorption and PL, respectively. In this case the FWHM reaches a value of 120 nm, doubling the value measured for CdSe QDs, denoting a stronger QD size dispersion for PbS QDs. Again, a larger Stokes shift is observed in the case of the PbS-PMMA nanocomposite as compared to the colloid. An average radius of 3.2 nm has been measured by transmission electron microscopy (TEM) for PbS QDs, which is consistent with published data [29].

4. Planar QD-PMMA Waveguides

PMMA is suitable polymer for integrated optics applications due to its trouble-free process and its transparency in the

(a)

— Colloidal

········ Composite

(b)
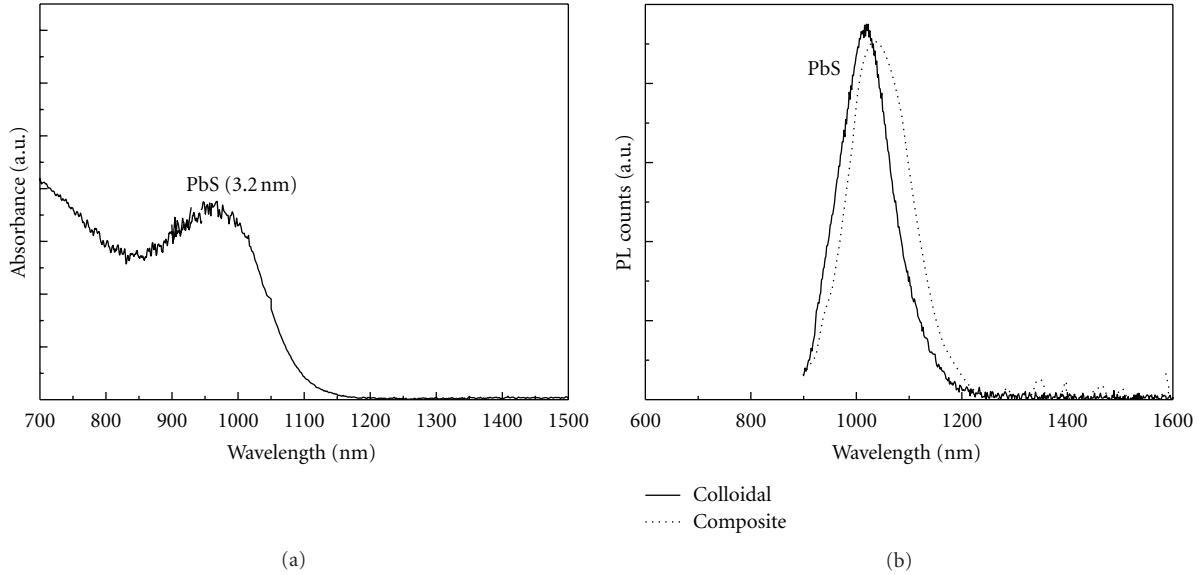
FIGURE 3: Absorption (a) and PL spectra (b) of colloidal PbS. Dot line shows PL spectra in the PMMA/NQD nanocomposite.

— PMMA

— PMMA + CdSe
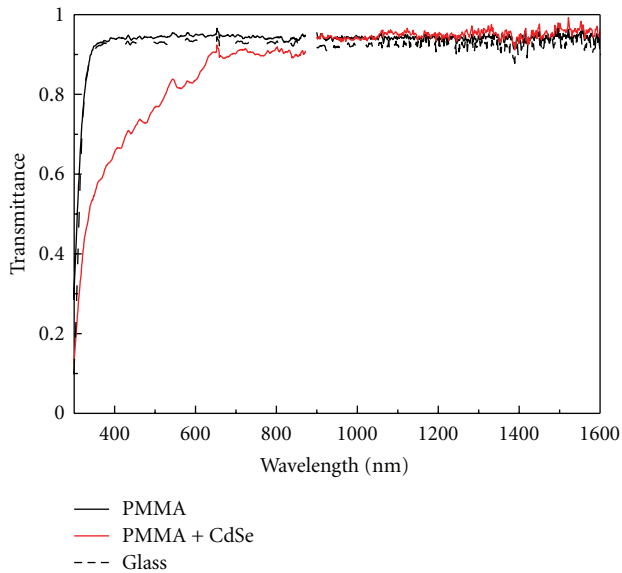
--- Glass

FIGURE 4: Transmittance spectrum of a $2\,\mu$m PMMA film spin coated on glass. Black and red lines correspond to PMMA and PMMA mixed with CdSe (filling factor of 0.02). Transmittance of glass is depicted with black dash lines.

visible and the infrared region. Figure 4 shows transmittance spectrum of a $2\,\mu$m PMMA film spin coated on glass (black line). Between 400 and 1500 nm, the absorption is almost that of the glass. Then, this polymer becomes an interesting material for waveguiding applications when it is deposited on a low index wafer (in this case SiO_2/Si). Moreover, PMMA is an appropriate host polymer for embedding oleate-capped QDs due to their adequate chemical interaction. This results in homogenous films, which suggests a great potentiality of these nanocomposites for photonic applications. In this

section waveguiding properties of PMMA doped with colloidal QDs will be discussed.

CdSe-PMMA waveguides have been thoroughly studied in [22] using samples with different QDs concentrations. As much as the concentration of nanoparticles is increased into the matrix, its refractive index becomes higher. However, for high filling factors $>10^{-3}$ of CdSe QDs in PMMA (filling factor is defined as the ratio between the volume occupied by QDs over the total volume), the QDs strongly attenuate the laser beam, and waveguiding is not possible. Red line of Figure 4 shows the transmittance spectrum of a $2\,\mu$m CdSe-PMMA film with a filling factor of 0.02. Transmittance drops to a value around 80% for 600 nm, the wavelength corresponding to the PL peak (ground exciton recombination). Since in a standard waveguide propagation length is usually around 1 cm, it is expected that the throughput of light at this wavelength will be nearly zero. Therefore, it is necessary to use QD-PMMA nanocomposites with quite lower filling factors (10^{-4}–10^{-3}) for maintaining small propagation losses (10–20 cm^{-1} for that range). Moreover, the PL of QDs can be also waveguided by pumping the QD-PMMA nanocomposite from the surface of the samples as well (see inset in Figure 1). In this work, we extrapolate these results to other QDs families (CdS, CdTe, and PbS), obtaining low propagation losses using similar filling factors. In the following sections a summary of different waveguides is presented.

4.1. CdSe-PMMA Waveguides. Figure 5 shows the guided-PL spectra of a CdSe-PMMA thin film by pumping the structure from the edges (continuous line) and from the surface (dash line) using a 404 nm GaN diode laser. The spectrum obtained by end fire coupling suffers an appreciable red-shift of the PL peak with respect to the one measured in the composite solution. This is probably due to a reabsorption effect of the
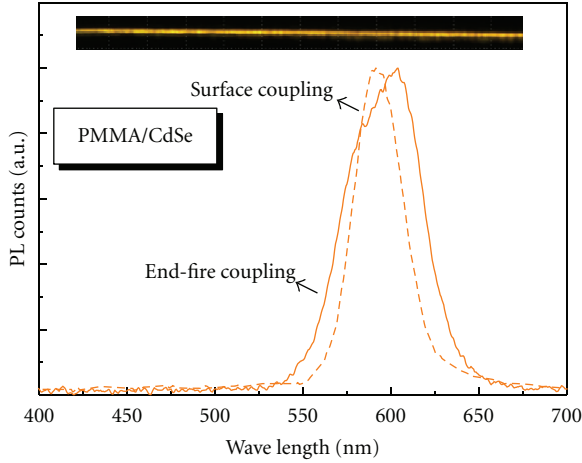
FIGURE 5: Waveguided PL spectrum of a PMMA/CdSe thin film obtained by end-fire coupling (continuous line) and top surface coupling (dashed line). The inset shows a picture of the waveguided PL at the output of the structure.
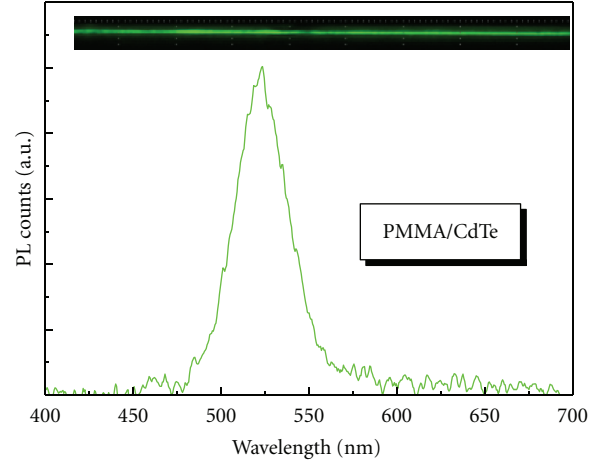
FIGURE 7: Waveguided PL band of a PMMA/CdTe thin film obtained by end-fire coupling. The inset shows a picture of the waveguided PL at the output face of the thin film.
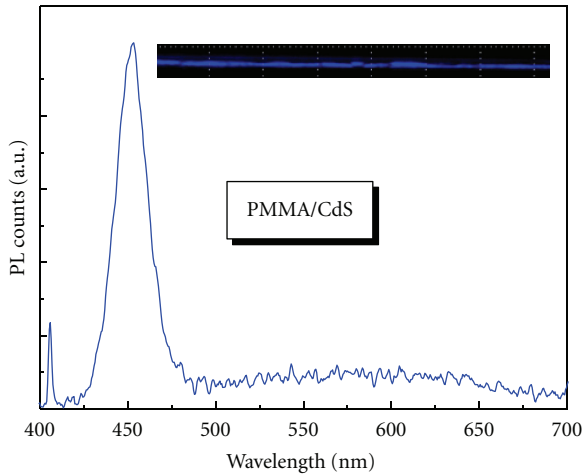
FIGURE 6: Waveguided PL spectrum of a PMMA/CdS waveguide obtained by surface coupling. The inset shows a photograph of the waveguided PL at the output of the structure.

FIGURE 8: Waveguiding PL spectrum of a PMM/PbS waveguide obtained by end-fire coupling.

wavelengths close to 580 nm, where the absorption exciton peak takes place. Furthermore, the PL band is broader than the one found in the colloid, maybe to different environment conditions [24]. However, when the sample is pumped from the surface, the guided PL is symmetric, centered at 591 nm and slightly narrower in comparison to the colloid PL, maybe because this sort of coupling allows a constant pumping in the whole length of the waveguide. The inset shows a picture of the orange guided PL due to CdSe QDs in PMMA.

4.2. CdS-PMMA Waveguides. **Figure 6** depicts the waveguided PL spectrum in a CdS-PMMA thin film pumping the structure from the top surface at 404 nm. In this case the PL band is centered at 453 nm and has a linewidth of 22 nm, so there is not a big difference with the PL band measured in the nanocomposite. We can also observe a broader and weaker PL band centered at around 620 nm corresponding

to surface states [5]. In the inset a picture of the blue guided-PL is shown.

4.3. CdTe-PMMA Waveguides. **Figure 7** shows the waveguided PL (see picture in the inset) measured in a CdTe-PMMA thin film by using end-fire pumping at 404 nm. The PL band is centered at 523 nm and has a linewidth of 35 nm, this time only 5 nm broader than the one found in the colloid. In this case the waveguided PL shows a symmetric peak because the absorption exciton peak is placed at longer wavelengths (537 nm, see **Figure 2(a)**), and hence the reabsorption of the guided PL is weaker.

4.4. PbS-PMMA Waveguides. **Figure 8** shows the waveguided PL of a PbS-PMMA thin film by using end-fire pumping at 633 nm (HeNe laser). In this case, the 404 nm wavelength (GaN laser diode) could not be used to pump the nanocomposite, because the absorption coefficient of PbS is too high

at this wavelength (see Figure 3). The PL band is centered at 1050 nm and its linewidth around 130 nm.

5. Perspectives

The fabrication of two-dimensional waveguides is of high interest for integrated photonic devices [30]. The integration of nanocrystal QDs in polymers (eventually photolithographic ones) opens a new method to implement hybrid organic-inorganic photonic and optoelectronic devices [31]. It has already been demonstrated amplification and lasing using PbSe QDs [32], CdSe-ZnS [33], and CdS-CdSe-ZnS [34] core-shell QDs dispersed in sol-gel films of TiO_2 and ZrO_2 planar waveguides. Then, it is expected that the polymer/NQD can be used for active purposes in waveguides [24], microcavities [22], and other photonic structures [23]. In addition taking in account that the emission wavelength can be tuned by changing the material forming the QDs and their size [14–20], it has demonstrated the applications of colloidal QDs in LEDs technology [35]. This property joined to the fact that it is possible to disperse several types of QDs into the matrix [36, 37], suggest the possibility to obtain white waveguided light; in a similar way that it is used in recent LED technology [38]. Finally, it has already studied the utility of colloidal QDs for sensing in optical fibers [39]. Then, QD-polymer waveguides can be applied to be a good probe for temperature sensing [40]. In this section we describe some preliminary results that illustrate the potential capabilities of these hybrid materials in next future.

5.1. Multicolor Waveguiding.
If one disperses QDs emitting at different wavelengths, into the same waveguide it is possible to obtain broad waveguided-PL spectra composed by the different "QD colors." In this case, it is critical to adjust the relative amounts of QDs into the matrix in order to avoid (or compensate) the reabsorption of light generated in QDs whose emission takes place at higher energies (shorter wavelengths) by QDs whose absorption and emission occur at lower energies (longer wavelengths). In [24] we proposed the inclusion of CdSe and CdTe in the same PMMA matrix. As a result the structure was able to waveguide the PL emitted from the two QD ensembles: green (535 nm) and orange (595 nm) colors corresponding to CdTe and CdSe QDs, respectively. Figure 9 shows the PL spectrum (hollow circles) of a similar structure able to guide three colors (see the three pictures at the top panel of Figure 9) by the dispersion of CdS (blue), CdTe (green), and CdSe (orange) QDs in the same matrix. The PL spectrum can be nicely reproduced by the sum of three Gaussian components (dashed lines) whose peaks take place at 452, 539, and 601 nm, corresponding to the CdS, CdTe, and CdSe QD ensembles, respectively. The PL tail observed at long wavelengths is associated to the surface states of CdS (see Figure 6).

5.2. Lithographic Nanocomposite.
One of the most interesting characteristics of polymers is the possibility to be patterned by different lithographic techniques. Among them UV
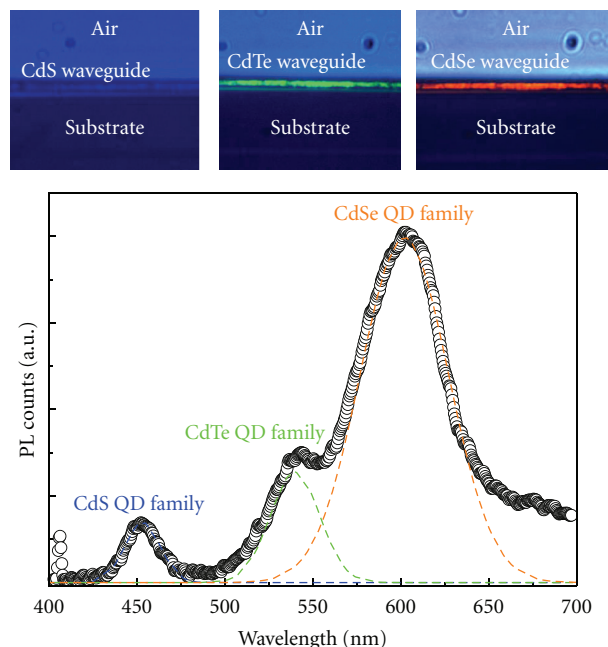
FIGURE 9: Waveguided PL spectrum in a nanocomposite thin film containing CdS, CdTe, and CdSe QDs. The pictures at the top panel show the three waveguided-PL components by using appropriate filters.

photolithography is the most appropriate for the fabrication of two-dimensional waveguides working in UV-VIS-NIR wavelengths because they require micropattern widths in the range 1–20 μm and high aspect ratios. Particularly, SU-8 is a commercially available photoresist and one of the most used for polymer based waveguiding applications [41, 42] because it is easily patternable by UV photolithography and has a high refractive index (around 1.5108 at 600 nm) [43]. Figure 10(a) shows the transmittance spectrum of a SU-8 film spin coated on a glass substrate. Between 600 and 1500 nm, the transmittance is similar to that of the bare glass, but below 600 nm the absorption increases due to its sensitivity to the UV radiation. As a result, SU-8 is an ideal candidate for hosting QDs, even if the main drawback lies in the poor chemical compatibility with as-synthesized QDs. The SU-8 photoresist is normally formulated with γ-butyrolactone or cyclopentanone, where oleate-capped QDs are not soluble. It is well known that surface modification of QDs may result in a change in the solubility properties of QDs [44]. In this way we propose a ligand exchange on oleate-terminated QDs to enhance their solubility in γ-butyrolactone [22]. Now, the resulting QDs are completely soluble in the SU-8 photoresist solution, and the nanocomposite with a homogeneous dispersion of CdSe QDs can be easily spin coated. Ridge waveguides based on the CdSe/SU-8 nanocomposite have been fabricated upon UV irradiation by using the procedure described in [43]. We observed that the lithographic performance of SU-8 was not disturbed by the presence of QDs. Moreover, as it was obtained in PMMA matrices, the concentration of QDs in SU-8 was
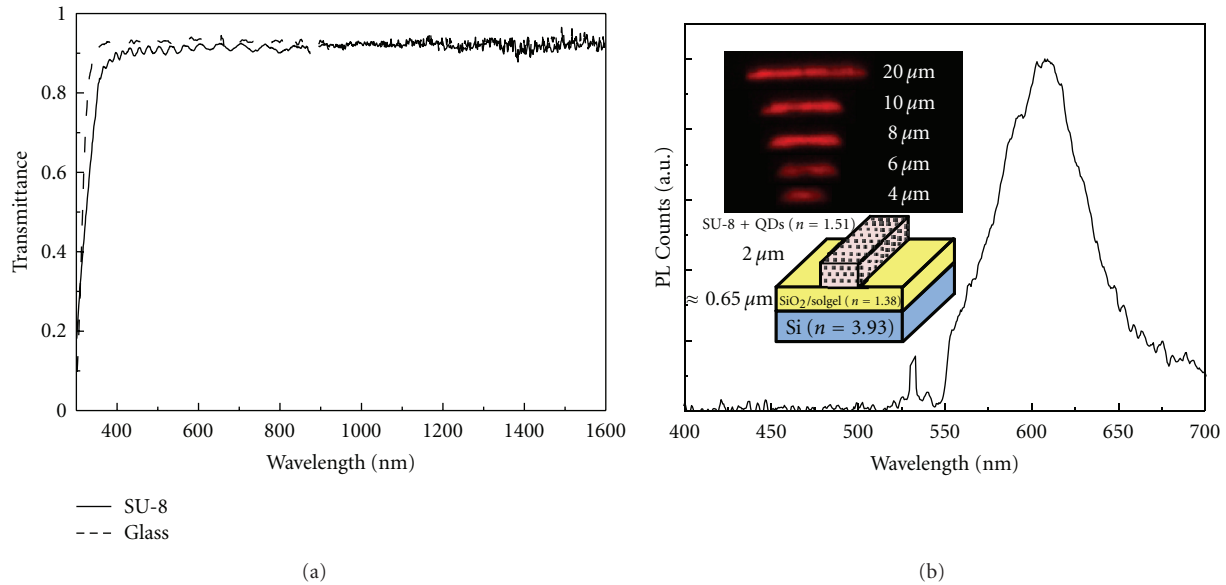
FIGURE 10: (a) Transmittance spectrua of a 2.5 μm SU-8 film spin coated on glass (continuous line) and that of the glass substrate itself (dashed line), (b) Waveguided-PL spectrum of a SU-8/CdSe ridge structure obtained by end-fire coupling. The insets show a picture of the waveguided PL at the output of ridge structure with different widths (above) and the scheme of the waveguide (below).

low enough to consider any refractive index increase of the matrix.

Waveguides were designed (see the inset in Figure 10(b)) to have widths between 4 and 20 μm and a height of 2.5 μm to guide the PL of CdSe QDs along the polymer ridges. PL light at the end of these waveguides (using end-fire pumping at 533 nm) is shown in the inset of Figure 10(b). The waveguided-PL band corresponding to CdSe QDs in a 8 μm SU-8 ridge (Figure 10(b)) has a peak centered at 610 nm and its linewidth is around 35 nm. The PL tail at longer wavelengths is due to the background fluorescence of the resist and its nature is explained in [24].

6. Conclusions

The integration of nanocrystal QDs in polymer matrices is an interesting approach for developing nanocomposites able to be used in new organic photonic devices. In this work, films made to be the dispersion of colloidal nanostructures (CdS, CdTe, CdSe and PbS) in a PMMA matrix are demonstrated to be a good core for waveguides. Using the appropriate concentrations of QD into the matrix, these films are able to waveguide the PL, and even more than one color when different types of QDs are embedded in the polymer. Then, these results are extrapolated to a photolithographic polymer (SU8), obtaining the waveguiding of the PL in a ridge waveguide fabricated by UV lithography. Finally, it is interesting to note that the polymers studied in this work show low transmission losses in the 600–1500 nm range. This feature, together with the possibility of tuned emission wavelength of colloidal QDs with their size or composition, makes these nanocomposites a suitable materials for waveguiding, not only for telecommunications applications (980, 1300, and 1500 nm) but also for the visible range.

References

[1] N. Tomczak, D. Jańczewski, M. Han, and G. J. Vancso, "Designer polymer-quantum dot architectures," *Progress in Polymer Science*, vol. 34, no. 5, pp. 393–430, 2009.

[2] M. A. Uddin and H. P. Chan, "Materials and process optimization in the reliable fabrication of polymer photonic devices," *Journal of Optoelectronics and Advanced Materials*, vol. 10, no. 1, pp. 1–17, 2008.

[3] M. A. Reilly, C. Marinelli, C. N. Morgan et al., "Rib waveguide dye-doped polymer amplifier with up to 26 dB optical gain at 625 nm," *Applied Physics Letters*, vol. 85, no. 22, article no. 3, pp. 5137–5139, 2004.

[4] K. C. Tsang, C. Y. Wong, and E. Y. B. Pun, "Eu³⁺-doped planar optical polymer waveguide amplifiers," *IEEE Photonics Technology Letters*, vol. 22, no. 14, pp. 1024–1026, 2010.

[5] L. Hu, H. Wu, L. Du, H. Ge, X. Chen, and N. Dai, "The effect of annealing and photoactivation on the optical transitions of band-band and surface trap states of colloidal quantum dots in PMMA," *Nanotechnology*, vol. 22, no. 12, Article ID 125202, 2011.

[6] R. Abargues, K. Abderrafi, E. Pedrueza et al., "Optical properties of different polymer thin films containing in situ synthesized Ag and Au nanoparticles," *New Journal of Chemistry*, vol. 33, no. 8, pp. 1720–1725, 2009.

[7] D. Amarasinghe, A. Ruseckas, G. A. Turnbull, and I. D. W. Samuel, "Organic semiconductor optical amplifiers," *Proceedings of the IEEE*, vol. 97, no. 9, pp. 1637–1650, 2009.

[8] I. J. Kramer and E. H. Sargent, "Colloidal quantum dot photovoltaics: a path forward," *ACS Nano*, vol. 5, no. 11, pp. 8506–8514, 2011.

[9] G. Konstantatos and E. H. Sargent, "Nanostructured materials for photon detection," *Nature Nanotechnology*, vol. 5, no. 6, pp. 391–400, 2010.

[10] R. Gradess, R. Abargues, A. Habbou et al., "Localized surface plasmon resonance sensor based on Ag-PVA nanocomposite thin films," *Journal of Materials Chemistry*, vol. 19, no. 48, pp. 9233–9240, 2009.

[11] I. De Leon and P. Berini, "Amplification of long-range surface plasmons by a dipolar gain medium," *Nature Photonics*, vol. 4, no. 6, pp. 382–387, 2010.

[12] J. M. Ruano-López, M. Aguirregabiria, M. Tijero et al., "A new SU-8 process to integrate buried waveguides and sealed microchannels for a Lab-on-a-Chip," *Sensors and Actuators, B*, vol. 114, no. 1, pp. 542–551, 2006.

[13] V. I. Klimov, "Nanocrystal quantum dots: from fundamental photophysics to multicolor lasing," *Los Alamos Science*, no. 28, pp. 214–220, 2003.

[14] A. P. Alivisatos, "Perspectives on the physical chemistry of semiconductor nanocrystals," *Journal of Physical Chemistry*, vol. 100, no. 31, pp. 13226–13239, 1996.

[15] Y. Chan, J. S. Steckel, P. T. Snee et al., "Blue semiconductor nanocrystal laser," *Applied Physics Letters*, vol. 86, no. 7, Article ID 073102, pp. 1–3, 2005.

[16] D. L. Ferreira, F. O. Silva, L. C. D. S. Viol et al., "Growth kinetics of CdTe colloidal nanocrystals," *Journal of Chemical Physics*, vol. 131, no. 8, Article ID 084712, 2009.

[17] Y. Chen, J. Herrnsdorf, B. Guilhabert et al., "Colloidal quantum dot random laser," *Optics Express*, vol. 19, no. 4, pp. 2996–3003, 2011.

[18] V. Sukhovatkin, S. Musikhin, I. Gorelikov et al., "Room-temperature amplified spontaneous emission at 1300 nm in solution-processed PbS quantum-dot films," *Optics Letters*, vol. 30, no. 2, pp. 171–173, 2005.

[19] Z. Wu, Z. Mi, P. Bhattacharya, T. Zhu, and J. Xu, "Enhanced spontaneous emission at 1.55 μm from colloidal PbSe quantum dots in a Si photonic crystal microcavity," *Applied Physics Letters*, vol. 90, no. 17, Article ID 171105, 2007.

[20] G. Chen, R. Rapaport, D. T. Fuchs et al., "Optical gain from InAs nanocrystal quantum dots in a polymer matrix," *Applied Physics Letters*, vol. 87, no. 25, Article ID 251108, pp. 1–3, 2005.

[21] J. Jasieniak, J. Pacifico, R. Signorini et al., "Luminescence and amplified stimulated emission in CdSe-ZnS-nanocrystal-doped TiO$_2$ and ZrO$_2$ waveguides," *Advanced Functional Materials*, vol. 17, no. 10, pp. 1654–1662, 2007.

[22] V. M. Menon, S. Husaini, N. Valappil, and M. Luberto, "Photonic emitters and circuits based on colloidal quantum dot composites," in *6th Quantum Dots, Particles, and Nanoclusters*, vol. 72224 of *Proceedings of SPIE*, pp. 1–8, January 2009.

[23] T. N. Smirnova, O. V. Sakhno, P. V. Yezhov, L. M. Kokhtych, L. M. Goldenberg, and J. Stumpe, "Amplified spontaneous emission in polymer-CdSe/ZnS-nanocrystal DFB structures produced by the holographic method," *Nanotechnology*, vol. 20, no. 24, Article ID 245707, 2009.

[24] I. Surez, H. Gordillo, R. Abargues, S. Albert, and J. Martínez-Pastor, "Photoluminescence waveguiding in CdSe and CdTe QDs-PMMA nanocomposite films," *Nanotechnology*, vol. 22, no. 43, Article ID 435202, 2011.

[25] W. W. Yu and X. Peng, "Erratum: formation of high-quality CdS and other II-VI semiconductor nanocrystals in noncoordinating solvents: tunable reactivity of monomers," *Angewandte Chemie*, vol. 46, no. 15, p. 2559, 2007.

[26] W. W. Yu, L. Qu, W. Guo, and X. Peng, "Experimental determination of the extinction coefficient of CdTe, CdSe, and CdS nanocrystals," *Chemistry of Materials*, vol. 15, no. 14, pp. 2854–2860, 2003.

[27] A. P. Demchenko, *Advanced Fluorescence Reporters in Chemistry and Biology III: Applications in Sensing and Imaging*, vol. 10, Springer, Berlin, Germany, 2011.

[28] H. Sharma, S. N. Sharma, G. Singh, and S. M. Shivaprasad, "Effect of ratios of Cd:Se in CdSe nanoparticles on optical edge shifts and photoluminescence properties," *Physica E*, vol. 31, no. 2, pp. 180–186, 2006.

[29] J. Tang, L. Brzozowski, D. A. R. Barkhouse et al., "Quantum dot photovoltaics in the extreme quantum confinement regime: the surface-chemical origins of exceptional air- and light-stability," *ACS Nano*, vol. 4, no. 2, pp. 869–878, 2010.

[30] G. Lifante, Ed., *Integrated Photonics, Fundamentals*, Wiley & Sons, 2003.

[31] J. Clark and G. Lanzani, "Organic photonics for communications," *Nature Photonics*, vol. 4, no. 7, pp. 438–446, 2010.

[32] R. D. Schaller, M. A. Petruska, and V. I. Klimov, "Tunable near-infrared optical gain and amplified spontaneous emission using pbse nanocrystals," *Journal of Physical Chemistry B*, vol. 107, no. 50, pp. 13765–13768, 2003.

[33] V. I. Klimov, A. A. Mikhailovsky, S. Xu et al., "Optical gain and stimulated emission in nanocrystal quantum dots," *Science*, vol. 290, no. 5490, pp. 314–317, 2000.

[34] J. J. Jasieniak, I. Fortunati, S. Gardin et al., "Highly efficient amplified stimulated emission from CdSe-CdS-ZnS quantum dot doped waveguides with two-photon infrared optical pumping," *Advanced Materials*, vol. 20, no. 1, pp. 69–73, 2008.

[35] Q. Sun, Y. A. Wang, L. S. Li et al., "Bright, multicoloured light-emitting diodes based on quantum dots," *Nature Photonics*, vol. 1, no. 12, pp. 717–722, 2007.

[36] J. Lee, V. C. Sundar, J. R. Heine, M. G. Bawendi, and K. F. Jensen, "Full color emission from II-VI semiconductor quantum dot-polymer composites," *Advanced Materials*, vol. 12, no. 15, pp. 1102–1105, 2000.

[37] S. Sapra, S. Mayilo, T. A. Klar, A. L. Rogach, and J. Feldmann, "Bright white-light emission from semiconductor nanocrystals: by chance and by design," *Advanced Materials*, vol. 19, no. 4, pp. 569–572, 2007.

[38] J. Park, J. Lee, and Y.-Y. Noh, "Optical and thermal properties of large-area OLED lightings with metallic grids," *Organic Electronics*, vol. 13, no. 1, pp. 184–194, 2012.

[39] P. Jorge, M. A. Martins, T. Trindade, J. L. Santos, and F. Farahi, "Optical fiber sensing using quantum dots," *Sensors*, vol. 7, no. 12, pp. 3489–3534, 2007.

[40] A. Bueno, I. Suárez, R. Abargues, S. Sales, and J. P. Martínez-Pastor, "Temperature sensor based on colloidal Quantum Dots-PMMA nanocompositewaveguides," *IEEE Sensors*. In press.

[41] N. Pelletier, B. Bêche, E. Gaviot et al., "Single-mode rib optical waveguides on SOG/SU-8 polymer and integrated Mach-Zehnder for designing thermal sensors," *IEEE Sensors Journal*, vol. 6, no. 3, pp. 565–570, 2006.

[42] B. S. Schmidt, A. H. J. Yang, D. Erickson, and M. Lipson, "Optofluidic trapping and transport on solid core waveguides within a microfluidic device," *Optics Express*, vol. 15, no. 22, pp. 14322–14334, 2007.

[43] http://www.microchem.com/Prod-SU8_KMPR.htm.

[44] C. B. Murray, C. R. Kagan, and M. G. Bawendi, "Synthesis and characterization of monodisperse nanocrystals and close-packed nanocrystal assemblies," *Annual Review of Materials Science*, vol. 30, pp. 545–610, 2000.